

KONINKRIJK DER



NEDERLANDEN

20. 08. 2004

(91)

Bureau voor de Industriële Eigendom



REC'D 27 SEP 2004

WIPO

PCT

Hierbij wordt verklaard, dat in Nederland op 12 augustus 2003 onder nummer 1024091,
ten name van:

AB SKF

te Göteborg (Zweden)

een aanvraag om octrooi werd ingediend voor:

"Sliding bearing with improved surface topography",

en dat de hieraan gehechte stukken overeenstemmen met de oorspronkelijk ingediende stukken.

Rijswijk, 18 augustus 2004

De Directeur van het Bureau voor de Industriële Eigendom,
voor deze,

mr. I.W. van der Eijk

**PRIORITY
DOCUMENT**SUBMITTED OR TRANSMITTED IN
COMPLIANCE WITH RULE 17.1(a) OR (b)

10 24091

Abstract

5 A sliding bearing comprises two opposite bearing surfaces which enclose a gap containing a lubricant film, said bearing surfaces being moveable with respect to each other in a generally parallel fashion, at least one of said surfaces being provided with at least one cavity, said cavity having a depth which is at least equal to the lubricant film thickness. The cavity depth is at least equal to 10 times the lubricant film thickness.

Sliding bearing with improved surface topography

The invention is related to the field of sliding bearing contacts. Such sliding contacts are present in various locations of all sorts of machinery, and in particular in the bearing components thereof. As an example, reference is made to the contact between the cage and the rolling elements of a bearing, or between the rolling elements and the flange of a bearing ring of a tapered roller bearing.

Generally, it is desirable to reduce the friction in such sliding bearing contacts. A reduced friction enhances bearing life due to the lower temperatures which are generated in service within the bearing contact. This has a favourable influence on the properties of the lubricant whereby the desired lubricant film thickness in the bearing contact can be maintained. Thus, wear of the surfaces in the sliding contact can be kept within acceptable limits.

The aim of the invention is to further improve the quality of bearings having a sliding contact. This aim is achieved by a sliding bearing contact comprising two opposite bearing surfaces which enclose a gap containing a lubricant film, said bearing surfaces being moveable with respect to each other in a generally parallel fashion, at least one of said surfaces being provided with at least one cavity, said cavity having a depth which is at least equal to the lubricant film thickness. Under running conditions, said lubricant film thickness may be in the range of 0,01 μm to 10 μm .

Preferably, the cavity depth is at least equal to 10 times the lubricant film thickness. Even better results are obtained in case the cavity depth is at least equal to 20 times the lubricant film thickness. A cavity depth up to 30 times the lubricant film thickness about represents the embodiment which still has a noticeable useful contribution to friction reduction.

Furthermore, it appears to be favourable in case the sum of the surface areas of all cavities of one and the same bearing surface amounts to at least 15% of the contact area of the bearing surfaces. On the other hand, the sum of the surface areas of all cavities of one and the same bearing surface should amount to at most 50% of the contact area of the bearing surfaces.

Furthermore, it appears to be useful in case the total cavity area is distributed over more than one cavity. Preferably, at least one of the surfaces has at least 4 cavities. Furthermore, at most 8 cavities should be applied.

In case one and only one cavity is provided, said cavity is preferably positioned approximately at equal distances from the inlet and the outlet.

In case at least two cavities are provided, the distance between the foremost cavity and the inlet is preferably larger than the distance between the rearmost cavity and the outlet. The center of a cavity or of a group of cavities may be located at a distance of 0.6 to 0.8 times the bearing length from the inlet.

The invention will now be described further with reference to several examples of a sliding bearing.

Figure 1 shows a longitudinal section through a linear wedge type sliding bearing according to the state of the art.

Figure 2 shows a longitudinal cross-section through a sliding bearing according to the invention.

Figure 3 shows a graph containing the pressure as function of the length along the bottom wall of the sliding bearing according to figure 2.

Figure 4 shows a graph containing the dependence of the friction coefficients on the depth of the cavity of the sliding bearing according to figure 2.

Figure 5 shows a graph containing the pressure distribution for all cases, as well as for the two-dimensional Reynolds case, along the lower surface.

Figure 6 shows a detail on a larger scale of figure 5.

Figure 7 shows a graph comparing the friction coefficients for all cases for both the top wall of the cavity parallel to the stationary upper surface and parallel to the lower, moving surface.

Figure 8 shows a graph containing the friction coefficient ratio for different positions of the cavity.

Figure 9 shows a graph containing the pressure distribution for all cases including the two-dimensional Reynolds case with the pocket in different positions.

Figure 10 shows a longitudinal cross-section through a sliding bearing with multiple cavities.

Figure 11 shows a graph containing the pressure distribution for cases with four pockets, including the two-dimensional Reynolds case, wherein the pocket area is 25% of the total area.

Figure 12 shows a top view of the upper wall of a three-dimensional embodiment of the sliding bearing according to the invention.

Figure 13 shows a graph containing the pressure distribution along the lower surface of the sliding bearing according to figure 12, for $y = 0$ m.

Figure 14 shows a further embodiment with two cavities.

Figure 15 shows a graph containing the pressure distribution for the embodiment of figure 14 along the lower surface for $y = 0$ m.

In figure 1, a so-called infinitely long linear wedge of a prior art sliding bearing is shown. This sliding bearing has a lower member 1 and an upper member 2, which define respectively a lower bearing surface 3 and an upper bearing surface 4. Between the surfaces 3, 4, a film 5 of a suitable lubricant, e.g. an oil, is enclosed. It is assumed that the lower member 1 moves into the right direction with respect to the upper member 2 in figure 1. As a result, there is a movement of the film 5 through the gap 6 defined between the members 1, 2. In particular, the lubricant film 5 moves through the gap 6 from the inlet 7 thereof towards the outlet 8.

As will be clear from figure 1, at the entrance 7 the maximum thickness of the film 5 is h_1 , and at the outlet 8 h_0 . The length of the sliding bearing and thus of the gap 6 is indicated by B . The velocity of the lower member 1 with respect to the upper member 2 is indicated by U . The Cartesian coordinates x and z have been indicated as well.

It is observed that figure 1 is related to a two-dimensional case, which means that no account is taken of the other Cartesian coordinate y .

The friction coefficient is defined as

$$\mu = \frac{F}{W}$$

and by expressing the friction coefficient through dimensionless values for load and friction, the following formula is obtained:

$$\mu = \frac{h_0}{B} \frac{F^*}{6W^*}$$

Figure 3 shows the pressures on the bottom wall for the two-dimensional linear wedge according to figure 1, both obtained from the prior art Reynolds' solution given

before as well as from numerical results obtained by computational fluid dynamics computations according to the invention.

In the embodiment according to figure 2, a cavity defined by a depth h_3 , is present in the upper surface 4. Table 1 provides the results for the case wherein the top wall 9 of the pocket 10 is parallel to the moving wall. Moreover, it has been assumed that the upper surface 4 of the gap 7 is parallel to the moving bottom wall 3. As there is no analytical solution for this geometry, only numerical results for the total load 16 and for the total friction 17 are available. These results are given in table 1. From this table 1 and from figure 4 it is clear that the friction coefficient drops as the height of the hollow h_3 increases.

Table 1

Height of the hollow [m]	Load [mPa]	Friction [mPa]	Dimless load	Dimless friction	Friction coeff.	Coeff. ratio
h_3	W/L	F/L	W^*	F^*	μ	μ/μ_{2DRey}
2D (Reynolds)	635544	154.518	0.0265	0.773	2.431e-4	1
2D(CFD)	630643	150.221	0.0263	0.751	2.382e-4	0.980
2D(CFD)	633435	152.435	0.0264	0.762	2.406e-4	0.990
2D(CFD)	634212	153.143	0.0264	0.766	2.415e-4	0.993
$3.5 \cdot 10^{-6}$	625077	144.771	0.0260	0.724	2.316e-4	0.953
$5 \cdot 10^{-6}$	618906	139.261	0.0258	0.696	2.250e-4	0.926
$5.5 \cdot 10^{-6}$	618006	138.751	0.0258	0.694	2.245e-4	0.923
$10 \cdot 10^{-6}$	612759	125.923	0.0255	0.630	2.055e-4	0.845
$12.5 \cdot 10^{-6}$	611860	120.851	0.0255	0.604	1.975e-4	0.812
$15 \cdot 10^{-6}$	611353	118.494	0.0255	0.592	1.938e-4	0.797
$20 \cdot 10^{-6}$	610857	115.625	0.0255	0.578	1.893e-4	0.779
$30 \cdot 10^{-6}$	610466	113.148	0.0254	0.566	1.853e-4	0.762
$40 \cdot 10^{-6}$	610340	112.56	0.0254	0.563	1.844e-4	0.759

In a further case, it is assumed that the top wall 9 of the cavity 10 is parallel to the stationary wall 4. The results of this case are presented in table 2.

Table 2

Height of the hollow [m]	Load [mPa]	Friction [mPa]	Dimless load	Dimless friction	Friction coeff.	Coeff. ratio
h_3	W/L	F/L	W^*	F^*	M	μ/μ_{2DRey}
0	634212	153.143	0.0264	0.766	2.42e-04	0.993
$3.5 \cdot 10^{-6}$	625196	144.504	0.026	0.723	2.31e-04	0.951
$5 \cdot 10^{-6}$	618963	139.932	0.0258	0.7	2.26e-04	0.93
$5.5 \cdot 10^{-6}$	617726	137.749	0.0257	0.689	2.23e-04	0.917
$10 \cdot 10^{-6}$	612755	124.579	0.0255	0.623	2.03e-04	0.836
$12.5 \cdot 10^{-6}$	611845	120.992	0.0255	0.605	1.98e-04	0.814
$15 \cdot 10^{-6}$	611395	118.595	0.0255	0.593	1.94e-04	0.798
$20 \cdot 10^{-6}$	610866	115.684	0.0255	0.578	1.89e-04	0.779
$30 \cdot 10^{-6}$	610485	113.177	0.0254	0.566	1.85e-04	0.763
$40 \cdot 10^{-6}$	610340	112.58	0.0254	0.563	1.85e-04	0.759

5 Figure 5 shows the pressure distribution along the bottom wall for all cases which are listed in table 1. Figure 6 shows the region around the maximum pressures of figure 5 on an enlarged scale.

10 Figure 7 shows a comparison between the friction coefficient for the case with the top wall 9 of the cavity 10 parallel to the stationary upper surface 4, and with the top wall 9 of the cavity 10 parallel to the moving lower surface 3. It is noted that in the case of shallow cavities minor differences occur between these cases, but that for the case of deep cavities 10 the results are very similar.

15 Furthermore, the effect of the location of the cavity 10 as defined by the distance B_1 has been studied. Table 3 shows the results for calculated load, friction and friction coefficient. From this table 3 it is clear that the position B_1 at which the friction coefficient is minimal is around the middle of the length of the gap 6. This effect is also clearly shown in figure 8.'

The pressure distribution for these cases and the two-dimensional Reynolds' case along the lower surface 3 is shown in figure 9.

Table 3

Position of the pocket [m]	Load [mPa]	Friction [mPa]	Dimless load	Dimless friction	Friction coeff.	Coeff. ratio
B_1	W/L	F/L	W^*	F^*	μ	μ/μ_{2DRey}
$0.25 \cdot 10^{-2}$	401814	101.185	0.0167	0.506	2.518e-4	1.036
$0.5 \cdot 10^{-2}$	482803	102.464	0.0201	0.512	2.122e-4	0.873
$0.75 \cdot 10^{-2}$	560142	105.37	0.0233	0.527	1.881e-4	0.774
$0.95 \cdot 10^{-2}$	604587	109.992	0.0252	0.550	1.819e-4	0.748
$1 \cdot 10^{-2}$	610340	112.580	0.0254	0.563	1.845e-4	0.759
$1.05 \cdot 10^{-2}$	612709	113.656	0.0255	0.568	1.854e-4	0.763
$1.10 \cdot 10^{-2}$	610825	115.214	0.0255	0.576	1.886e-4	0.776
$1.25 \cdot 10^{-2}$	566752	110.209	0.0236	0.551	1.945e-4	0.800

- 5 In the case of figure 2, a single cavity 10 is present in the stationary upper surface 4, covering about 25% of the total length B of the sliding bearing. In a further case shown in figure 10, four cavities 9 having a length B_p have been applied, also covering about 25% of the total length B of the sliding bearing. The cavities are evenly spaced at distances B_f . Three different cases have been studied, each having an other distance B_1 for the first cavity 10 from the inlet 7 of the gap 6. The results for these three cases are presented in table 4.
- 10

Table 4

Position of the pocket [m]	Load [mPa]	Friction [mPa]	Dimless load	Dimless friction	Friction coeff.	Coeff. ratio
B_1	W/L	F/L	W^*	F^*	μ	μ/μ_{2DRey}
$1.875 \cdot 10^{-3}$ even spacing	487415	112.161	0.0203	0.561	2.301e-4	0.947
$2.5 \cdot 10^{-3}$	472362	102.226	0.0197	0.511	2.164e-4	0.890
$7 \cdot 10^{-3}$	580376	109.345	0.0241823	0.546726	1.884e-4	0.775

The pressure distribution for these three cases along the lower surface 4 is presented in figure 11, together with the two-dimensional Reynolds case. It is clear that a smaller distance B_1 from the first pocket 10 to the inlet 7 does not lead to a reduction in the friction coefficient.

A further case was studied, provided with eight pockets 10 having a length B_p which total to about 50% of the length B of the sliding bearing. Table 5 shows that such geometry does not lead to further reduction of the friction coefficient.

10

Table 5

Position of the pocket [m]	Load [mPa]	Friction [mPa]	Dimless load	Dimless friction	Friction coeff.	Coeff. ratio
B_1	W/L	F/L	W^*	F^*	μ	μ/μ_{2DRey}
$5 \cdot 10^{-6}$	353811	115.498	0.0147	0.577	$3.264e-4$	1.343
$10 \cdot 10^{-6}$	333489	102.951	0.0139	0.515	$3.087e-4$	1.270
$20 \cdot 10^{-6}$	325079	87.594	0.0135	0.438	$2.694e-4$	1.108
$40 \cdot 10^{-6}$	322323	79.137	0.0134	0.396	$2.455e-4$	1.010

The previous studies have all been related to two-dimensional cases. Subsequently, the behaviour of a three-dimensional linear wedge sliding bearing with a single cavity is studied. The lay-out in top view thereof is shown in figure 12. Reference L indicates the bearing width. L_1 defines the distance of the cavity 10 from the lateral boundary of the sliding bearing gap 6, L_p defines the width of the cavity 10. The following magnitudes have been selected:

$$B = L = 2 \cdot 10^{-2} \text{ m}, B_p = L_p = 1 \cdot 10^{-2} \text{ m}, L_1 = 0.5 \cdot 10^{-2} \text{ m}.$$

Table 6 shows the results of the varying distance B_1 . The pressure distribution along the lower surface for $y = 0 \text{ m}$ is shown in figure 13.

Table 6

Position of the pocket [m]	Load [mPa]	Friction [mPa]	Dimless load	Dimless friction	Friction coeff.	Coeff. ratio
B_1	W/L	F/L	W^*	F^*	μ	μ/μ_{2DRey}
0	275882	150.011	0.0115	0.750	5.438e-4	1
$5 \cdot 10^{-3}$	219692	118.527	0.0092	0.593	5.395e-4	0.992
$7.5 \cdot 10^{-3}$	242436	116.481	0.0101	0.582	4.805e-4	0.884
$7.7 \cdot 10^{-3}$	242467	116.192	0.0101	0.581	4.792e-4	0.881
$8 \cdot 10^{-3}$	241370	115.671	0.0101	0.5784	4.792e-4	0.881
$8.5 \cdot 10^{-3}$	234995	114.561	0.0098	0.573	4.875e-4	0.896

Finally, the embodiment of figure 14 has been studied in which two pockets of similar form and dimensions are applied. These dimensions are:

$$B = L = 2 \cdot 10^{-2} \text{ m}, L_p = 2 \cdot B_p = 1 \cdot 10^{-2} \text{ m}, L_1 = 0.5 \cdot 10^{-2} \text{ m}.$$

Table 7 shows the results of varying distances B_1 and B_2 , figure 15 the pressure distribution along the lower surface for $y = 0$ m.

10

Table 7

Position of the first pocket [m]	Gap between the pockets [m]	Load [mPa]	Friction [mPa]	Dimless load	Dimless friction	Friction coeff.	Coeff. ratio
B_1	B_2	W/L	F/L	W^*	F^*	μ	μ/μ_{3D}
0	0	275882	150.011	0.0115	0.750	5.438e-4	1
$5 \cdot 10^{-3}$	$2.5 \cdot 10^{-3}$	230303	117.07	0.0096	0.585	5.083e-4	0.935
$6 \cdot 10^{-3}$	$1 \cdot 10^{-3}$	236121	117.376	0.0098	0.587	4.971e-4	0.914
$6.5 \cdot 10^{-3}$	$1 \cdot 10^{-3}$	237723	116.784	0.0099	0.584	4.912e-4	0.903
$6.5 \cdot 10^{-3}$	$1.5 \cdot 10^{-3}$	234126	116.147	0.0098	0.581	4.961e-4	0.912
$7 \cdot 10^{-3}$	$1 \cdot 10^{-3}$	236597	116.021	0.0099	0.580	4.904e-4	0.902
$8 \cdot 10^{-3}$	$0.5 \cdot 10^{-3}$	233085	114.82	0.0097	0.574	4.926e-4	0.906

Although in the description given before as well as in the figures reference is made to a wedge with non-parallel bearing surfaces, the invention is also related to parallel bearing surfaces.

5

NOTATION

	h_1	maximum film thickness (see Fig. 1)
	h_0	minimum film thickness
10	h_3	height of the hollow (see Fig. 2)
	B	bearing length
	L	bearing width
	U	velocity in the x direction of the bottom wall
	x,y,z	Cartesian coordinates
15	t	time (s)
	p	pressure
	ρ	density
	η	dynamic viscosity
	ν	kinematic viscosity $\nu = \eta/\rho$
20	W	total load
	F	total friction
	W^*	dimensionless load
	F^*	dimensionless friction

25 MAIN VALUES

	B	$=$	$2 * 10^{-2} \text{ m}$
	U	$=$	1 m/s
	h_0	$=$	$1 * 10^{-6} \text{ m}$
30	h_1	$=$	$2 * 10^{-6} \text{ m}$
	ρ	$=$	103 kg/m^3
	η	$=$	10^{-2} Pas
	ν	$=$	$10^{-5} \text{ m}^2/\text{s}$

Claims

1. Sliding bearing comprising two opposite bearing surfaces (3, 4) which enclose a gap (6) containing a lubricant film (5), said bearing surfaces (3, 4) being moveable
5 with respect to each other in a generally parallel fashion, at least one (4) of said surfaces being provided with at least one cavity (10), said cavity having a depth which is at least equal to the lubricant film thickness.
2. Bearing according to claim 1, wherein the cavity depth is at least equal to 10
10 times the lubricant film thickness.
3. Bearing according to claim 2, wherein the cavity depth is at least equal to 20 times the lubricant film thickness.
4. Bearing according to claim 3, wherein the cavity depth is maximally 50 times
15 the lubricant film thickness.
5. Bearing according to any of the preceding claims, wherein the sum of the surface areas of all cavities of one and the same bearing surface amounts to at least
20 15% of the contact area of the bearing surfaces.
6. Bearing according to any of the preceding claims, wherein the sum of the surface areas of all cavities (10) of one (4) and the same bearing surface amounts to at most 50% of the contact area of the bearing surfaces (3, 4).
25
7. Bearing according to any of the preceding claims, wherein at least one of the surfaces (3, 4) has at least 4 cavities.
8. Bearing according to any of the preceding claims, wherein at least one of the
30 surfaces (3, 4) has at most 8 cavities.
9. Bearing according to any of the preceding claims, wherein the gap (6) between the bearing surfaces (3, 4) as seen in the direction of relative movement has an inlet (7)

and an outlet (8) for the lubricant film, whereby a bearing length is defined between said inlet (7) and outlet (8) and said inlet (7) and outlet (8) being at a distance from any of the cavities (10).

5 10. Bearing according to claim 9, wherein the center of a cavity (6) or of a group of cavities is located at a distance of 0.6 to 0.8 times the bearing length from the inlet (7).

10 11. Bearing according to claim 9, wherein one and only one cavity (6) is provided, said cavity being positioned approximately at equal distances from the inlet (7) and the outlet (8).

15 12. Bearing according to claim 9 or 10, wherein at least two cavities (6) are provided, the distance between the foremost cavity (10) and the inlet (7) being larger than the distance between the rearmost cavity (10) and the outlet (8).

 13. Bearing according to any of the preceding claims, wherein the cavities (10) are isolated from each other.

20 14. Bearing according to any of the preceding claims, wherein the lubricant film thickness under running conditions is in the range of 0,01 μm to 10 μm .

Fig 1

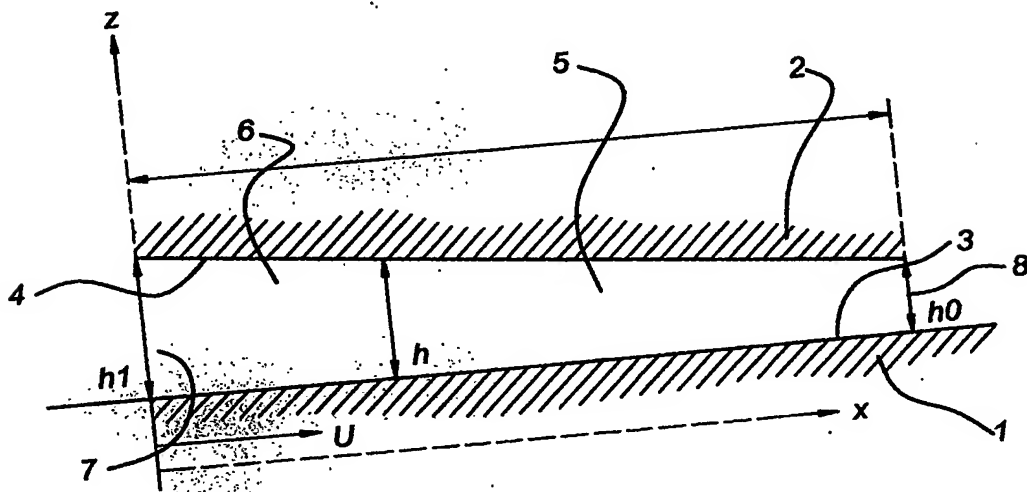


Fig 2

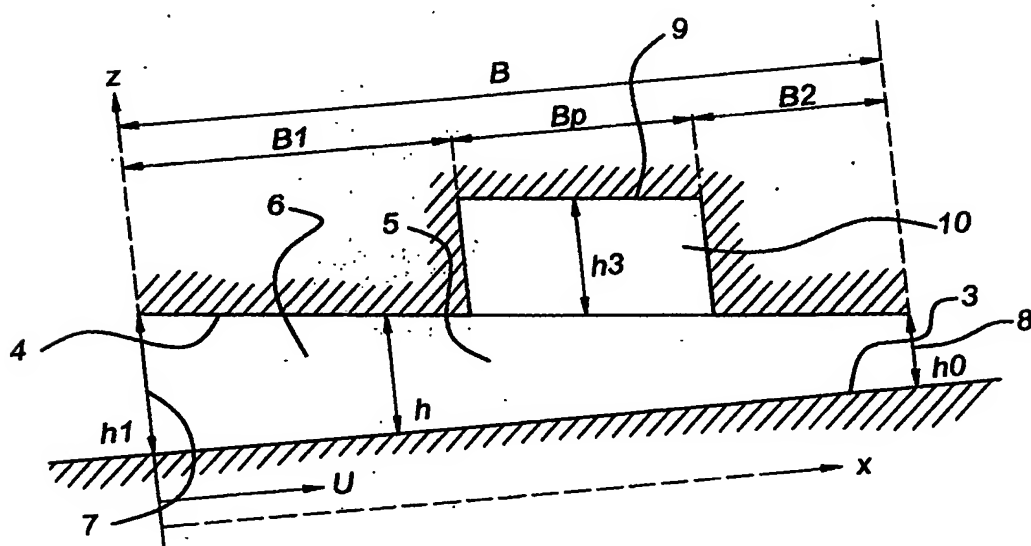


Fig 3

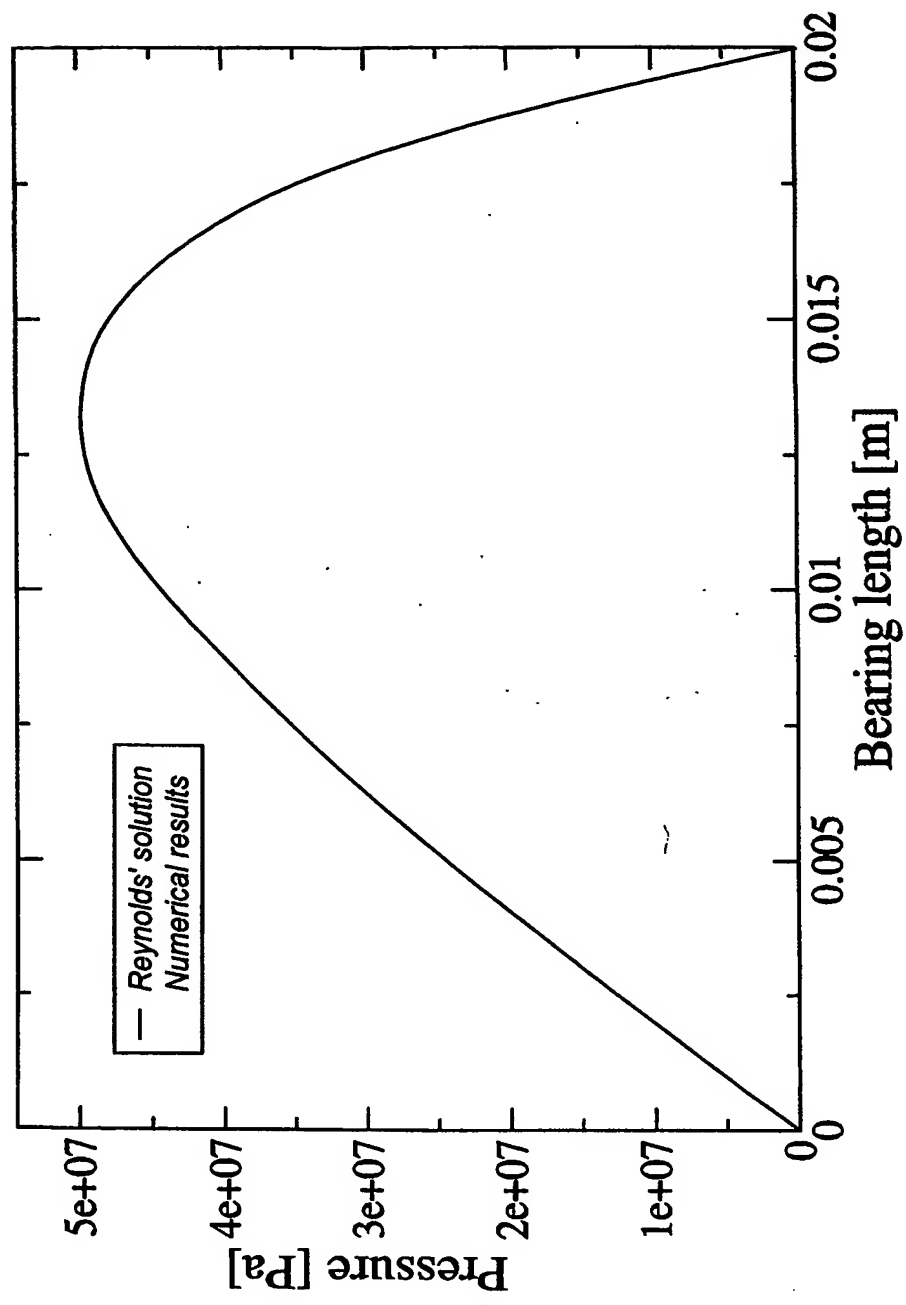


Fig 4

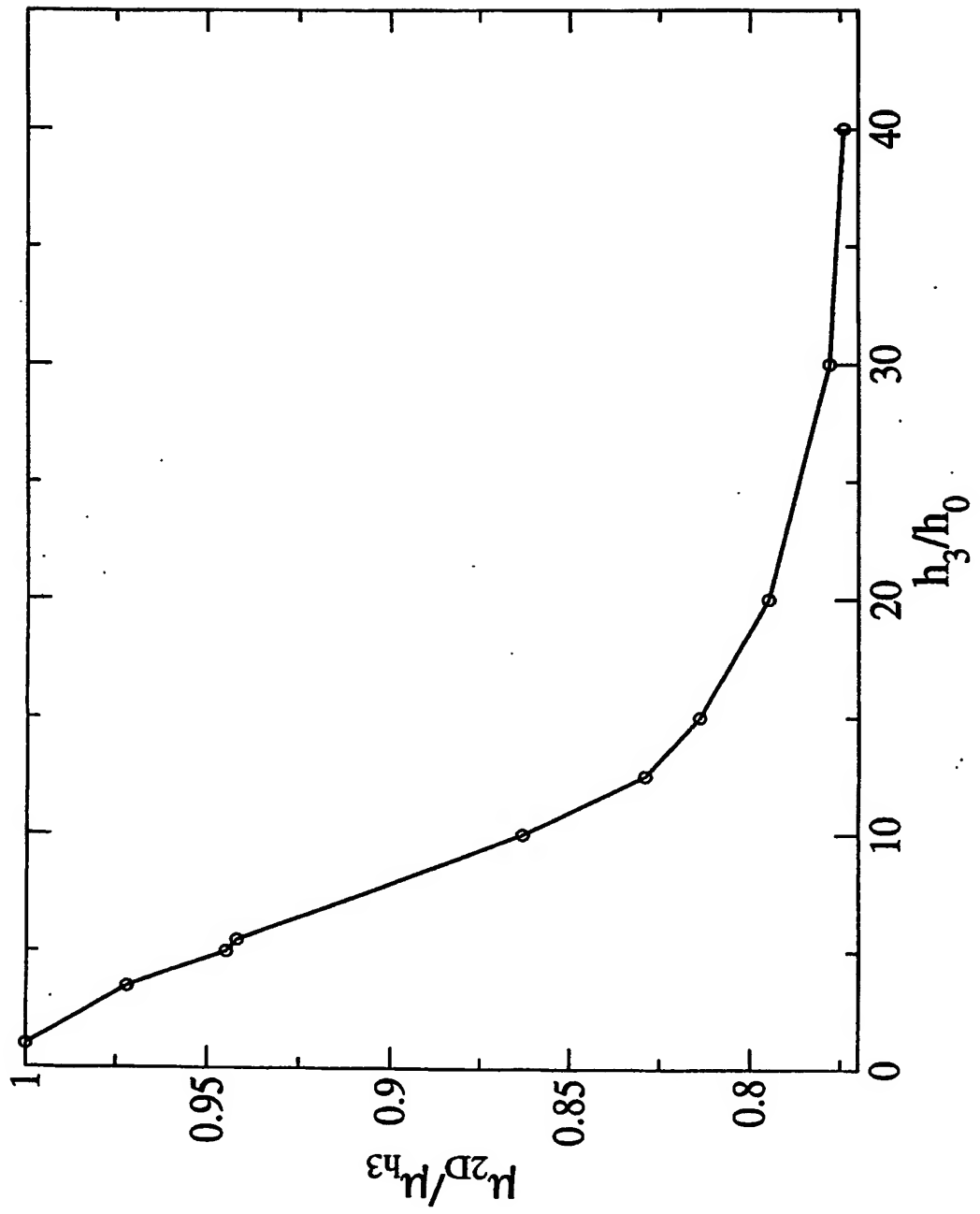


Fig 5

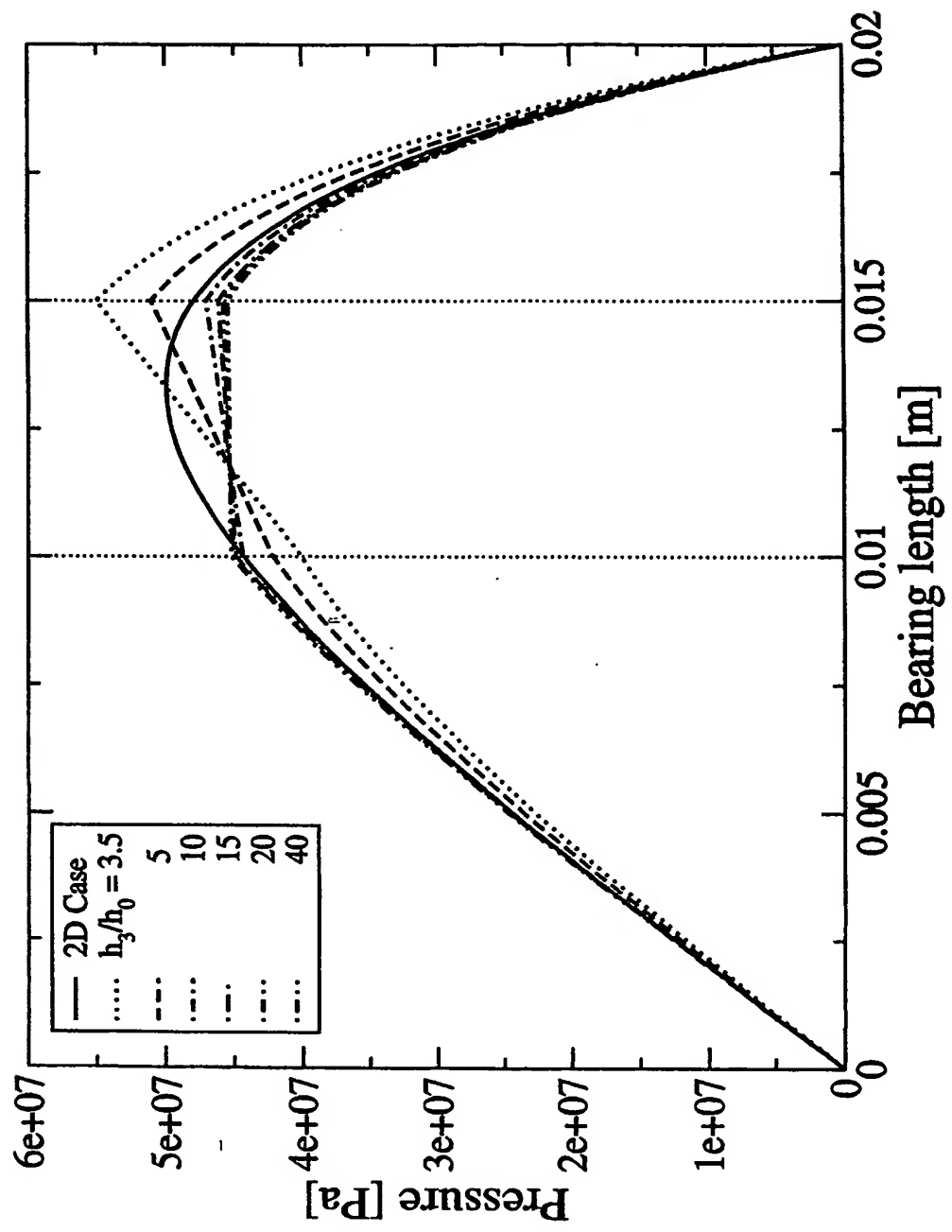


Fig 6

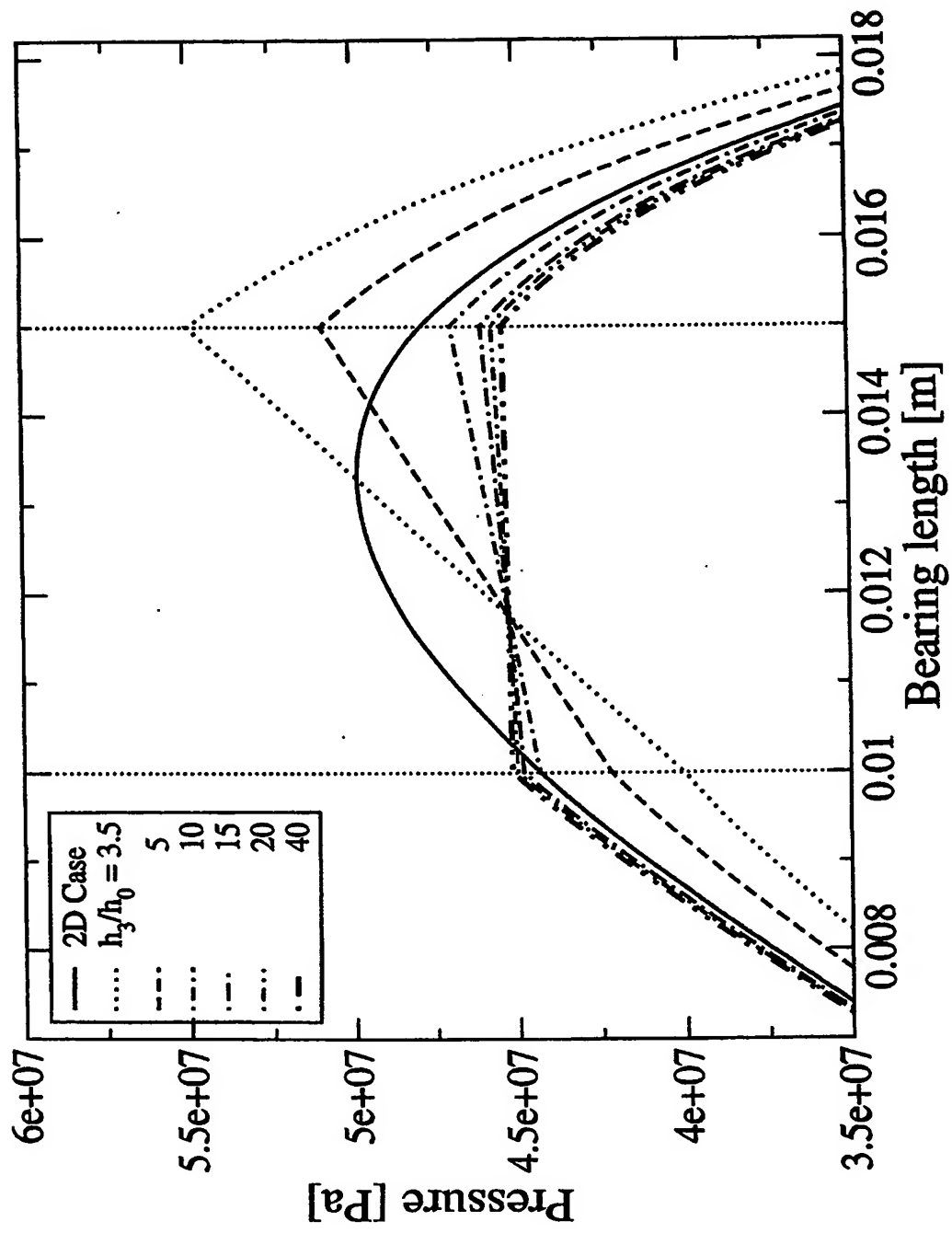


Fig 7

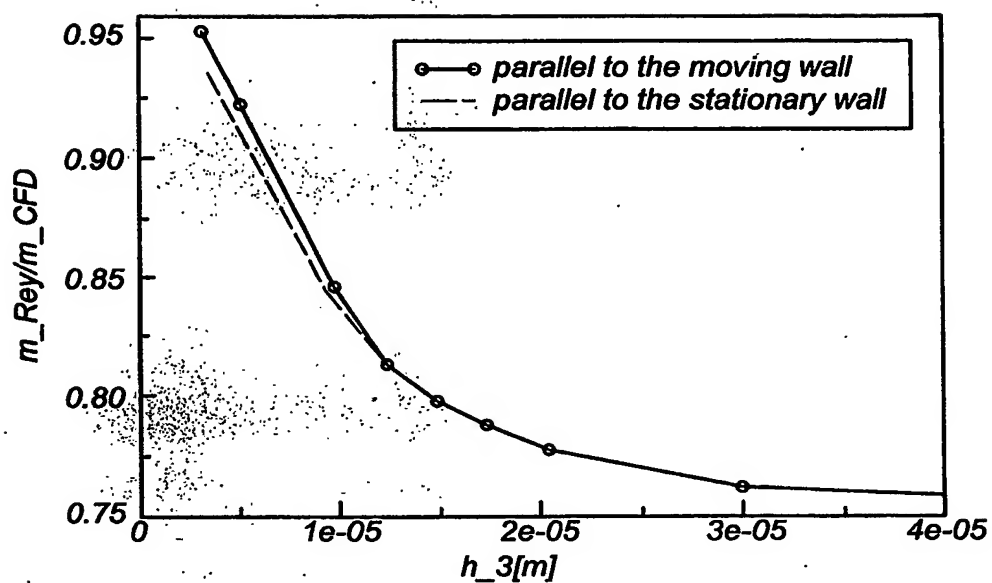


Fig 8

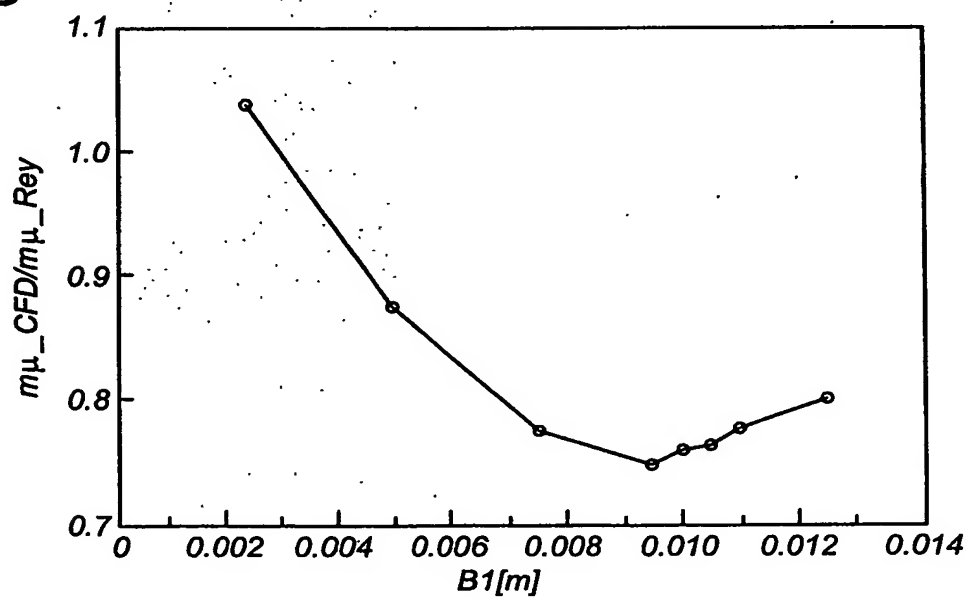


Fig 9

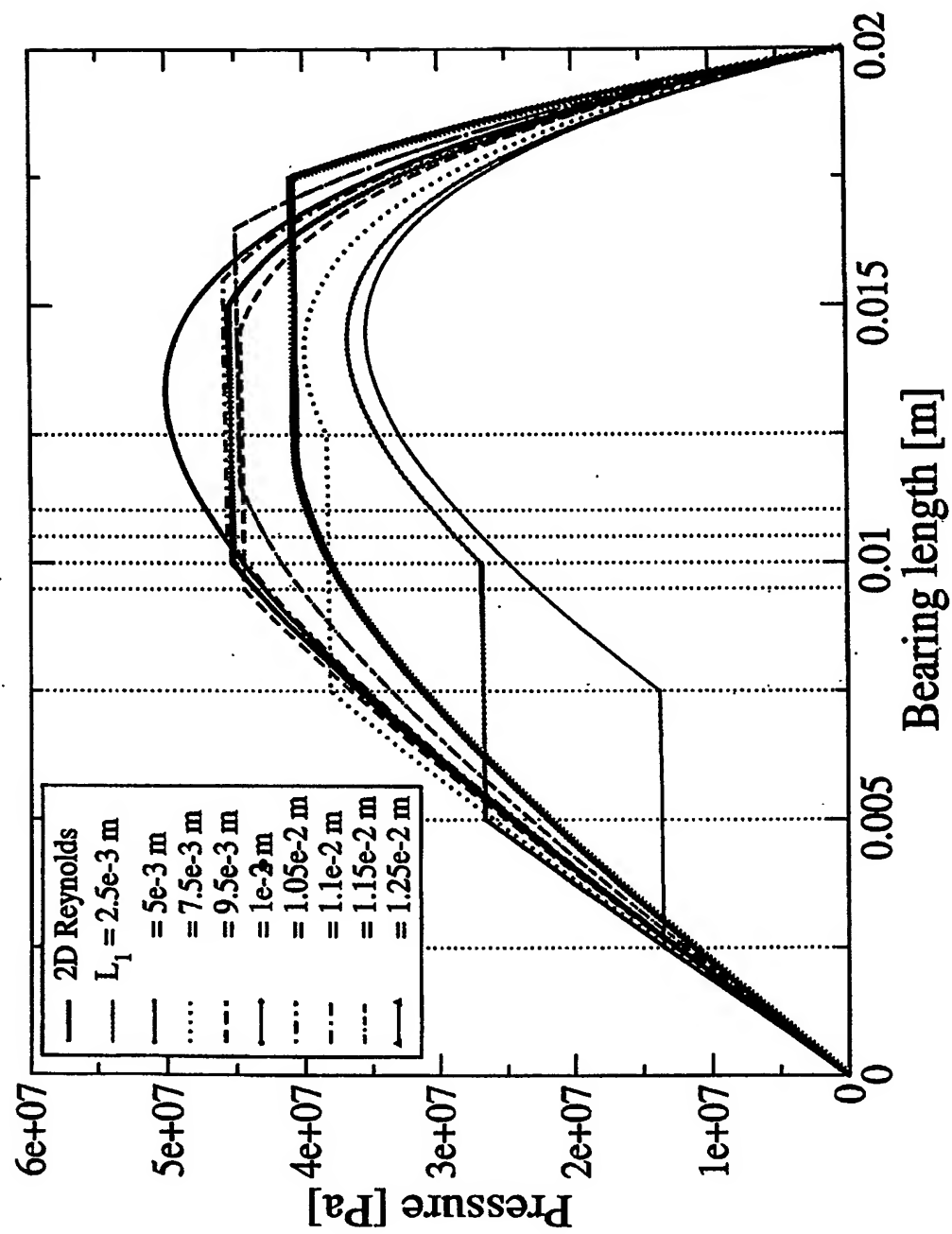


Fig. 10

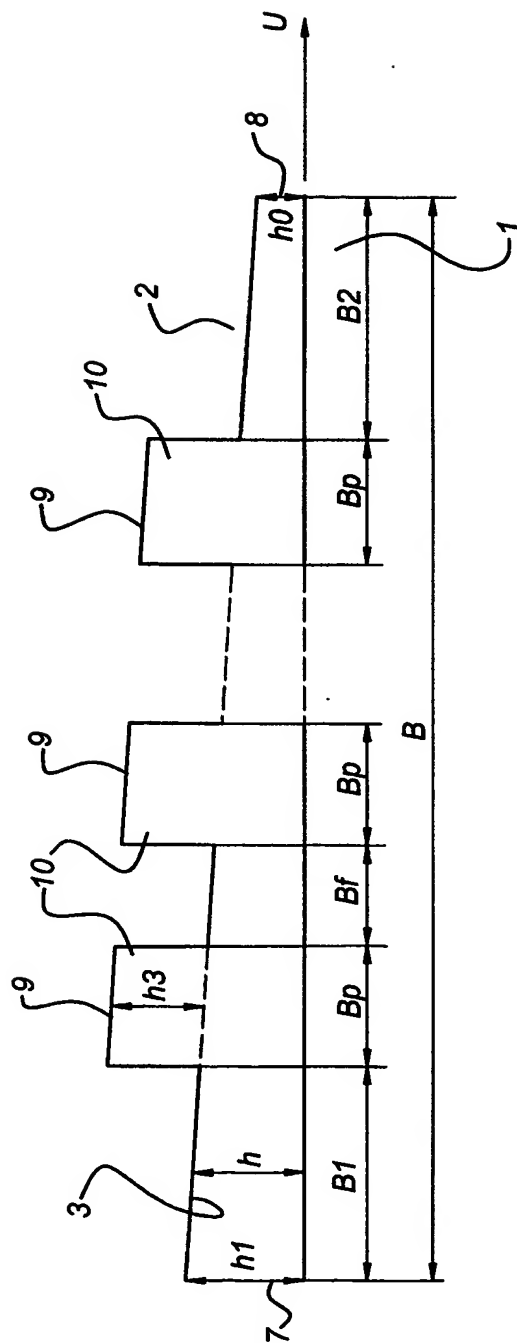


Fig 11

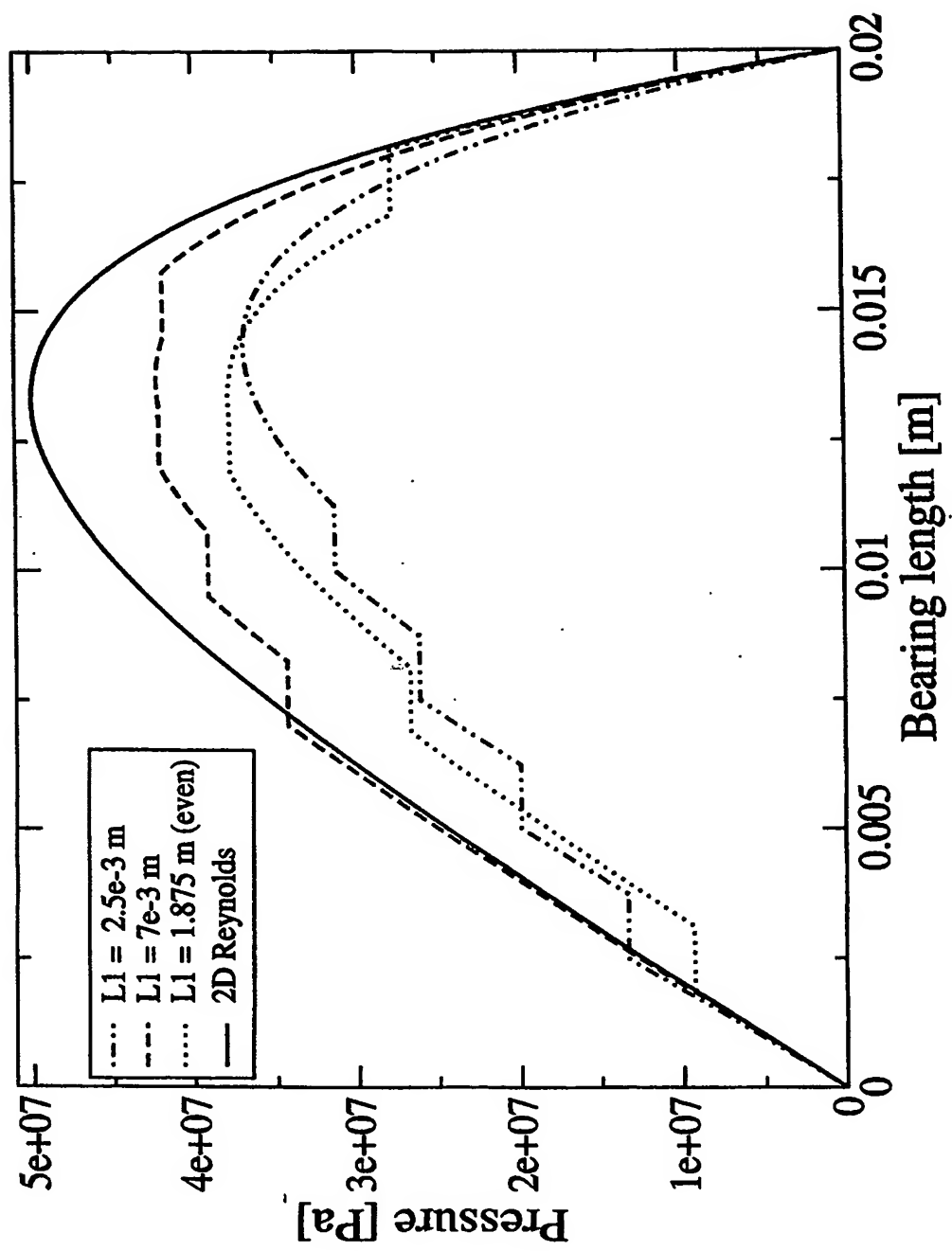


Fig 12

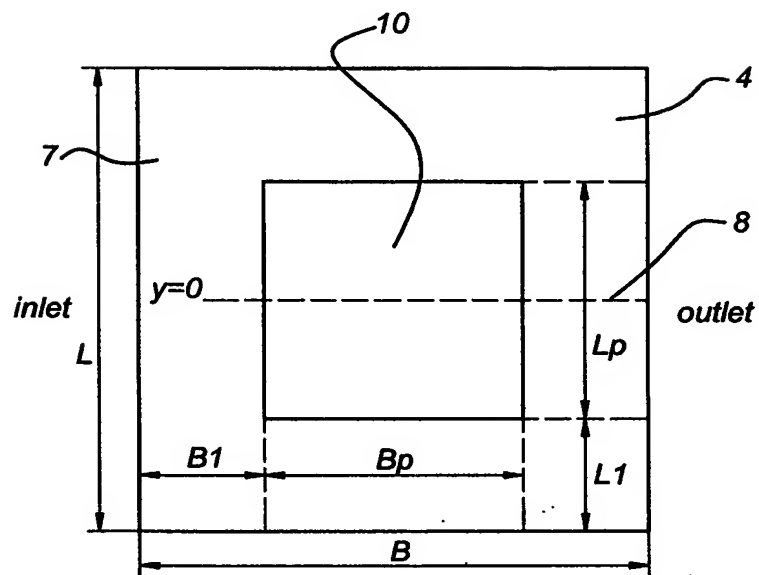


Fig 14

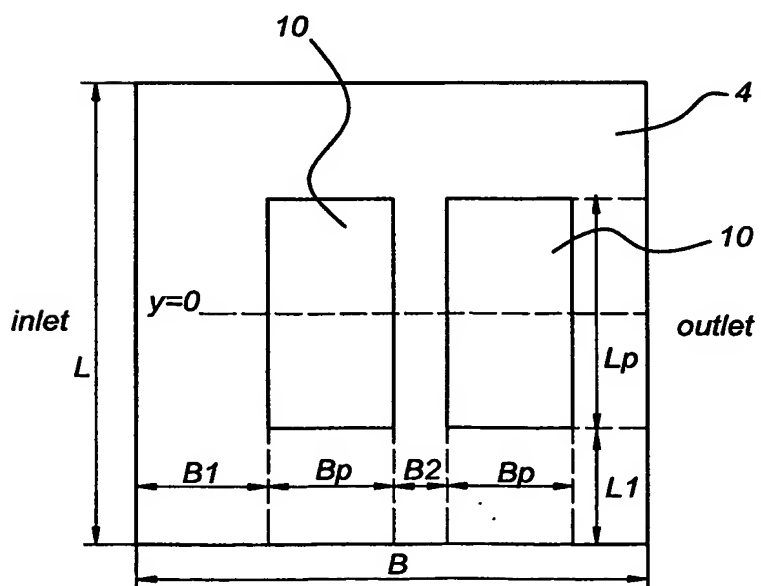


Fig 13

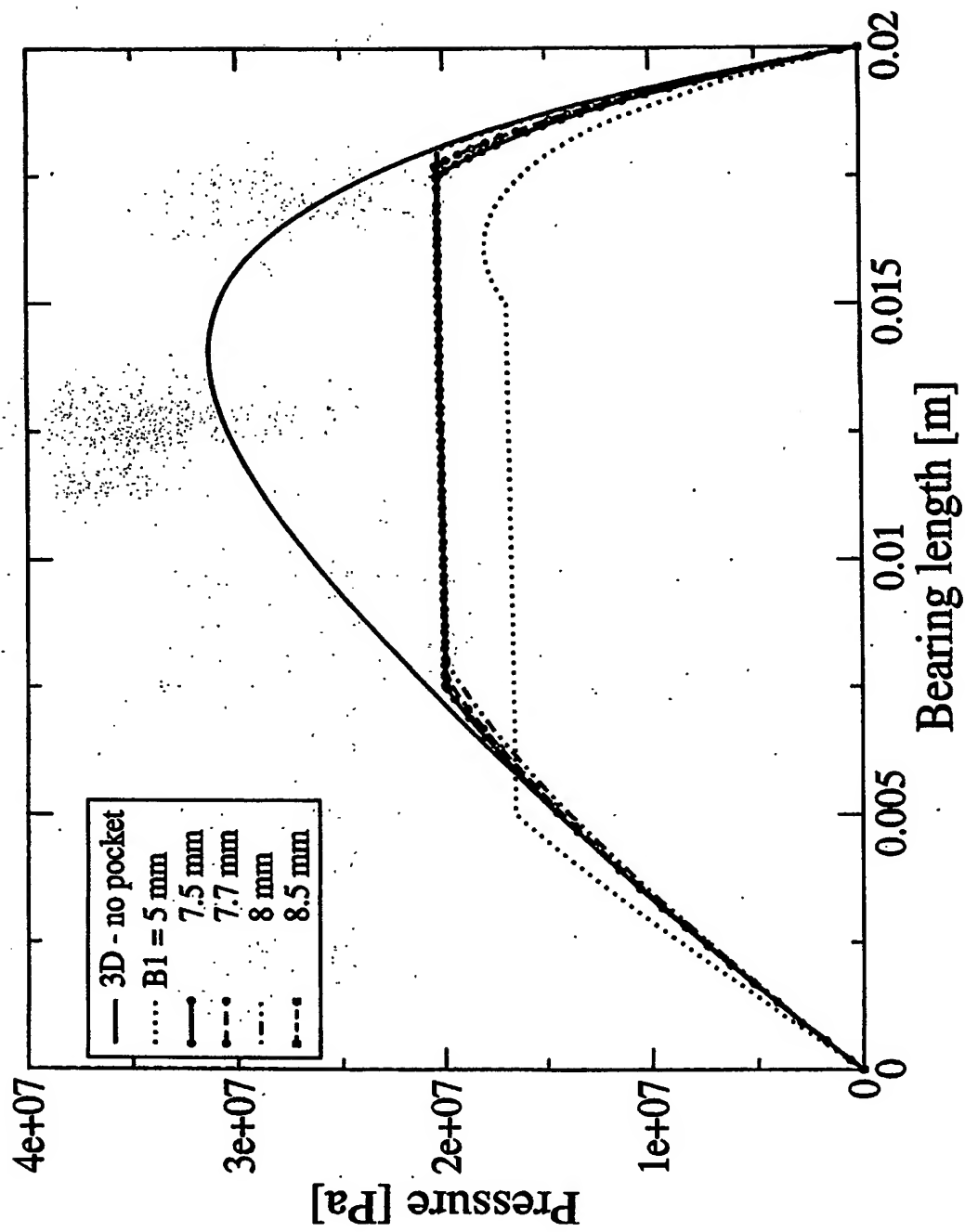


Figure 10 is a line graph showing Pressure [Pa] versus Bearing length [m]. The y-axis ranges from 0 to 4e+07 Pa, and the x-axis ranges from 0 to 0.02 m. The graph compares a 3D model (solid line) with various 2D models (dotted, dashed, and dash-dot lines with different markers). The 3D model shows a peak pressure of approximately 3.5e+07 Pa at a bearing length of about 0.012 m. The 2D models show lower peak pressures, ranging from approximately 1.5e+07 Pa to 2.5e+07 Pa, with peaks occurring at different bearing lengths between 0.01 and 0.015 m.

Bearing length [m]	3D Pressure [Pa]	2D Model 1 (B1=5e-3m, B2=2.5e-3m) Pressure [Pa]	2D Model 2 (B1=6e-3m, B2=1e-3m) Pressure [Pa]	2D Model 3 (B1=6.5e-3m, B2=1e-3m) Pressure [Pa]	2D Model 4 (B1=6.5e-3m, B2=1.5e-3m) Pressure [Pa]	2D Model 5 (B1=8e-3m, B2=0.5e-3m) Pressure [Pa]	2D Model 6 (B1=7e-3m, B2=1e-3m) Pressure [Pa]
0.000	0	0	0	0	0	0	0
0.005	~1.5e+07	~1.5e+07	~1.5e+07	~1.5e+07	~1.5e+07	~1.5e+07	~1.5e+07
0.010	~3.0e+07	~1.8e+07	~1.8e+07	~1.8e+07	~1.8e+07	~1.8e+07	~1.8e+07
0.012	~3.5e+07	~2.0e+07	~2.0e+07	~2.0e+07	~2.0e+07	~2.0e+07	~2.0e+07
0.015	~3.0e+07	~1.8e+07	~1.8e+07	~1.8e+07	~1.8e+07	~1.8e+07	~1.8e+07
0.020	0	0	0	0	0	0	0

